Journal of Science and Transport Technology
Journal homepage: https://jstt.vn/index.php/en

Estimation of the bond strength between FRP and concrete using ANFIS and hybridized ANFIS machine learning models

Thuy-Anh Nguyen, Hai-Bang Ly*
University of Transport Technology, 54 Trieu Khuc, Thanh Xuan, Hanoi 100000, Vietnam

Article info
Type of article:
Original research paper

DOI:
https://doi.org/10.58845/jstt.utt.2021.en.1.1.34-44

***Corresponding author:**
E-mail address:
banglh@utt.edu.vn

Received: 13/10/2021
Revised: 30/11/2021
Accepted: 02/12/2021

Abstract: Adaptive Neuro-Based Fuzzy Inference System (ANFIS) and Particle Swarm Optimization (PSO) algorithms were utilized to produce numerical tools for predicting the bond strength between the concrete surface and carbon fiber reinforced polymer (CFRP) sheets. From the relevant literature, a credible database encompassing 242 test specimens was developed, along with six input factors that primarily determine bond strength. These characteristics include the beam's width, the compressive strength of the concrete, the FRP thickness, the FRP modulus of elasticity, the FRP length, and the FRP width. Finally, using conventional statistical metrics, the outputs of the two suggested models (ANFIS and ANFIS-PSO) were compared to the experimental data. Both models were shown to be a good alternative strategy for predicting the bond strength of FRP-to-concrete.

Keywords: Bond Strength; FRP-to-concrete; Adaptive Neuro-Based Fuzzy Inference System (ANFIS); Particle Swarm Optimization (PSO).

1. Introduction

Reinforced concrete is one of the most commonly used construction materials because of its strength, ease of application, adaptability, flexibility, durability, and affordable price. However, in complicated weather conditions, intense aggressiveness of the environment causes steel rusting, peeling of the protective concrete layer, and reducing the reinforced concrete bearing structure system [1]. In addition, the changes due to user requirements often tend to be detrimental to existing structures requiring the implementation of solutions to repair, upgrade or even replace the structure. At that time, repairing and upgrading are often practical solutions because replacing a series of works requires significant costs. Therefore, the development of repair and reinforcement technology solutions to maintain and restore the normal working of reinforced concrete structures is highly necessitated.

In recent times, repairing and reinforcing works by using fiber reinforced polymers (FRP) in sheet form is a solution that has been widely studied and applied [2,3]. This method takes advantage of the properties of FRP materials such as high strength and corrosion resistance, high durability, non-magnetic, and has a higher strength-to-weight ratio, which reduces the self-weight of an RC structure and high fatigue resistance. In addition, the convenience of construction, high aesthetics, ensuring the preservation of the old structural shape (because FRP sheets can be quickly bonded with structures of any cross-section), suitable for projects that

require high waterproofing and corrosion resistance is also an advantage to use reinforced FRP sheets outside the structure [4,5]. External reinforcement using FRP sheets is mainly reliant on the capacity of the FRP sheets to adhere to the concrete surface. This bond plays an essential role in stress transfer between the concrete and the FRP sheets and is critical in controlling various bondage failures in FRP-reinforced structures [6].

Many studies have investigated the bond strength using experimental approaches such as the break test or the single ring shear test [7–9]. In addition, to calculate the bond strength of FRP-to-concrete, numerical approaches [10,11] and hybrid models expanded by experimental data and analytical solutions [12,13] have been utilized. Furthermore, based on empirical analysis of experimental data acquired from tensile testing, many distinct design equations have been constructed to estimate the bond strength [14–16]. However, multiple studies have shown that the capacity to forecast the bond strength of FRP-to-concrete is limited by the data sets employed [17,18]. Additionally, the aforementioned formulae do not take into account the nonlinear relationship between the input and output parameters and do not test for alternative combinations of input parameters when calculating bond strength. Furthermore, the majority of existing prediction algorithms overlook the adhesive material's characteristics [19].

Recent years have seen a progressive increase in popularity and the use of machine learning (ML) or artificial intelligence (AI) based on computer science. In the construction sector, machine learning or artificial intelligence has been used in areas such as structure [20,21], materials [22,23], soil mechanics [24,25]. As a result, artificial intelligence may be used to assess the bond strength of FRP-to-concrete. The Adaptive Neuro-Based Fuzzy Inference System (ANFIS) model, a branch of artificial intelligence, is commonly used in construction engineering. Therefore, the ANFIS model is suggested in this work to forecast the bond strength of FRP-to-concrete. In addition, the ANFIS model's hyperparameters are optimized using the Particle Swarm Optimization (PSO) technique. The following sections of the paper are given in chronological order: The theoretical foundation of the ANFIS model utilized in this work is introduced in section 2, the database for training and validation of ANFIS models is shown in part 3, and the findings and comments are presented in section 4. Finally, in section 5, some conclusions are presented.

2. Methods used

2.1. Adaptive Neuro-Based Fuzzy Inference System

Jang created the Adaptive Neural Fuzzy Inference System (ANFIS) in 1993 [26], which is a prominent artificial intelligence system that combines artificial neural networks with fuzzy logic. ANFIS uses fuzzy learning rules in the form of TSK (Takasi – Sugeno – Kang). The jth fuzzy learning rule of ANFIS is Rj of the form:

$$\text{IF: } X_1 \text{ is } B_1^j \text{ AND } X_2 \text{ is } B_2^j \ldots \text{AND } X_n \text{ is } B_n^j$$
$$\text{THEN: } Y = F_j = p_0^j + \sum_{i=1}^{n} p_i^j X_i \quad (1)$$

with X_i, Y are input and output variables respectively,

$B_1^j(x_i)$ are fuzzy linguistic variables corresponding to the input variable X_i, $p_i^j \in R$ is the coefficient of the linear function f_j, i = 1,2,…,n; j = 1,2,…,M

The structure of ANFIS consists of five layers [27] represented by several nodes and node functions (Fig 1). Various types of buttons, such as square and circular, are used to represent different aspects of adaptive learning. Parameters are present in square nodes (adaptive nodes), but not in round nodes (fixed nodes). Each button has a certain purpose. The direction of the signal is indicated by the link between two nodes. Buttons in the same class have the same function, as described below.

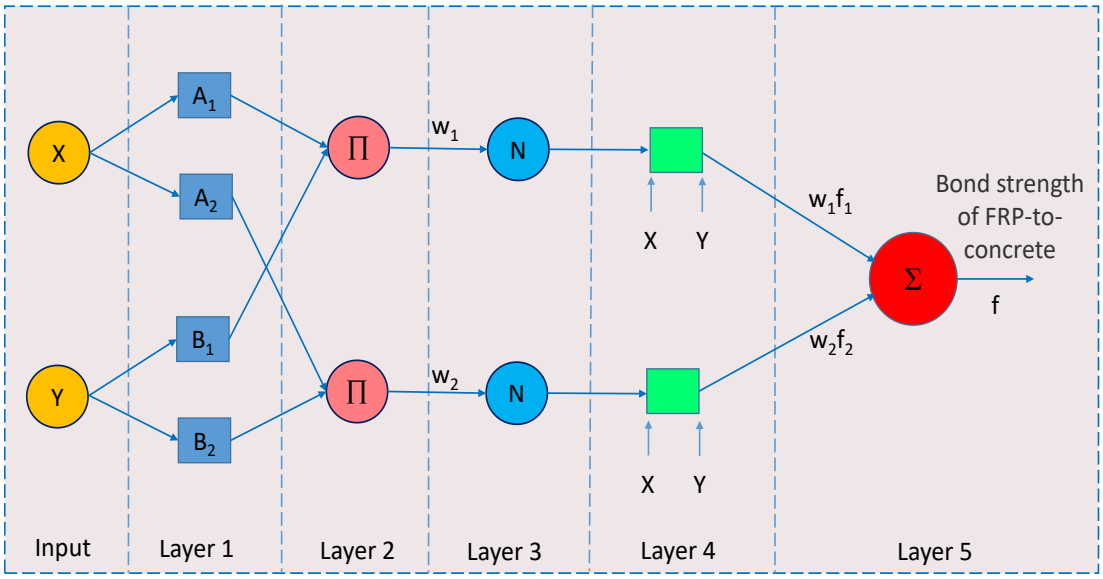

Fig. 1. The adaptive neuro-fuzzy inference (ANFIS) algorithm structure

- The first layer includes adaptive nodes (square nodes), as well as a membership function $\mu A_i^j(X_i)$. The output of this class is computed using the Gaussian membership function.

$$\mu_{gaussian}(x) = \exp\left[-\left(\frac{x-c_k}{s_k}\right)^2\right] \quad (2)$$

- The rule layer is the second layer. Each node in this layer is identified by a circle labeled Π, referred to as rule nodes. It is the sum of the incoming signals, and the output value of each node indicates the strength of a rule:

$$\omega_i = \eta_{B_i}(X)\eta_{C_i}(Y) \quad (3)$$

- Each node in the third tier is a fixed circular node designated N. The ith node in this class is defined as the ratio of the ith rule's magnitude to the total of all normals' intensities:

$$\bar{\omega}_i = \frac{\omega_i}{\sum_i \omega_i} \quad (4)$$

- Each node in the fourth layer, denoted Z, is a square adaptive node. This layer has the same number of nodes as the third layer. Each node outputs the weighted result value of a particular rule:

$$\bar{\omega}_i F_i = \bar{\omega}_i(p_i X + q_i Y + r_i) \quad (5)$$

- The fifth layer has a circular node. In this layer, the symbol ∑ is the output equal to the sum of all input signals.

$$\sum_i \bar{\omega}_i F_i = \frac{\sum_i \omega_i F_i}{\sum_i \omega_i} \quad (6)$$

2.2. Particle Swarm Optimization Algorithm

The Particle Swarm Optimization method (PSO) was created by Eberhart and Kennedy (1995) [28]. It is a population-based stochastic optimization approach that replicates the behavior of flocks of birds or schools of fish hunting for food. They proposed that the swarm foraging process occurs in an area of space where all components in the swarm are aware of the location of food and maintain their position closest to it. Then, the greatest strategy for finding food is to follow the flock's leaders - those closest to the food. The PSO algorithm is offered to adapt to this circumstance and solve optimization difficulties. Each answer in PSO is a component of the preceding scenario. Each element is defined by two parameters: its current location and velocity. Simultaneously, each element has a fitness value, which the fitness function evaluates. At the start, the swarm, or more accurately, the location of each element, is initialized randomly. During motion, each element is impacted by two pieces of information: the first, named Qbest, is the element's best position in the past; the second, designated Jbest, is the swarm's best position in the past. Specifically, after each discrete time period, each element's velocity and

location are changed using the following formulas:

$$V_{i,m}^{(t+1)}=W.V_{i,m}^{(t)}+C_1.rand().\left(Qbest_{i,m}-X_{i,m}^{(t)}\right) +C_2.rand().\left(Jbest_{i,m}-X_{i,m}^{(t)}\right) \quad (7)$$

$$V_{i,m}^{(t+1)}=W.V_{i,m}^{(t)}+C_1.rand().\left(Qbest_{i,m}-X_{i,m}^{(t)}\right) +C_2.rand().\left(Jbest_{i,m}-X_{i,m}^{(t)}\right) \quad (8)$$

2.3. Cross-validation

Cross-validation is a statistical technique that is used to quantify the performance (or accuracy) of machine learning models. It guards against model overfitting, which is particularly important when data is few.

The critical parameter in this technique is k, representing the number of groups into which the training dataset will be divided. Then, the testing data section will be kept separate and reserved for the final evaluation step to check the "reaction" of the model when encountering completely unseen data. The training data will be randomly divided into k parts (k is an integer or preferably a given value of 5 or 10 [29,30]. In the next step, the model is trained k times. For each simulation, the process will choose 1 part as validation data and k-1 as training data. The final model evaluation result will be the average of the evaluation results of k training times, which allows one to evaluate the predictive models more objectively and accurately.

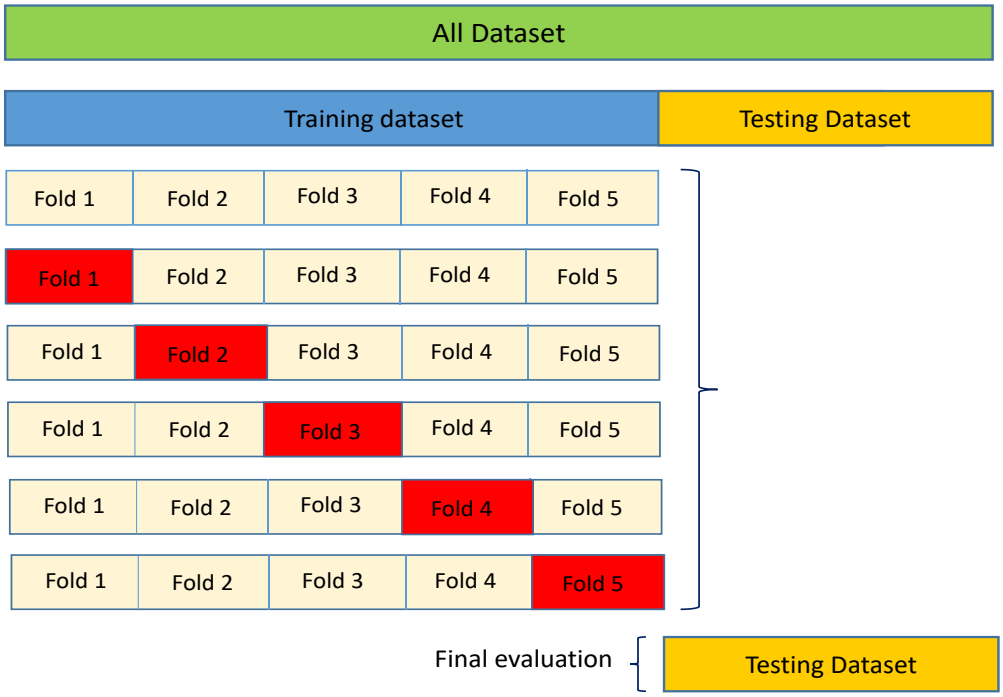

Fig. 2. Demonstration of 5 fold cross-validation technique

2.4. Model evaluation

The correlation between the predicted values by the machine learning model and the actual experimental values was evaluated using conventional assessment metrics such as Pearson correlation coefficient (R), root mean square error (RMSE), and mean absolute error (MAE) in this work. In general, the model's performance improves when the MAE and RMSE approach zero. Similarly, R's value is in the range [-1; 1], and the closer R's absolute value is to 1, the more accurate the model is. Formulas for calculating R, RMSE, and MAE can be found in the cited documents [31-33].

3. Database construction

The suggested ANFIS model for predicting FRP-to-concrete bond strength is based on a database of 242 laboratory test results from 15 published papers [6-8,34-42]. The experimental database is collected from the tests conducted to measure the bond strength between CFRP sheets and the concrete surface under direct tension. The training and testing datasets are randomly selected

from the database. 70% of the dataset is utilized for training, whereas 30% is used for testing the model. According to published experimental data, the bond strength between the CFRP panels and the concrete surface is mostly determined by the six primary factors used to build the ANFIS model. The beam width (b_c), the concrete compressive strength (f_c'), the FRP thickness (t), the FRP modulus of elasticity (E_f), the FRP length (l_f), and the FRP width (b_f).

Table 1 details the input and output parameters' notation, roles, and statistical analysis (minimum, maximum, mean, median, and standard deviation). The data distribution of input and output parameters and their occurrence frequency in the dataset, and the correlation relationship between the parameters are shown in Fig 3. The dotted line in Fig 3 shows the correlation graph between the pairs of parameters. Besides, the specific correlation values between the pairs of parameters are also shown. The parameters in the collected data set have low correlation (correlation value is less than 0.6), some pairs of parameters have very low correlation (correlation value is close to 0). The six input parameters of the dataset could thus be considered independent variables.

Table 1. Statistical analysis of the input and output variables used in this study

Variable	Not.	Min	Median	Mean	Max	Standard deviation	Skewness
I_1	b_c	100.000	150.000	158.884	400.000	47.797	1.431
I_2	f'_c	16.000	30.000	33.172	61.500	10.575	0.553
I_3	b_f	10.000	40.000	44.391	150.000	24.874	1.328
I_4	t_f	0.080	0.413	0.670	3.400	0.555	0.431
I_5	E_f	22.500	210.000	191.998	300.000	59.532	-0.453
I_6	L	50.000	147.500	156.628	500.000	83.921	1.537
Y	Pu	4.110	11.560	14.921	54.680	10.194	1.489

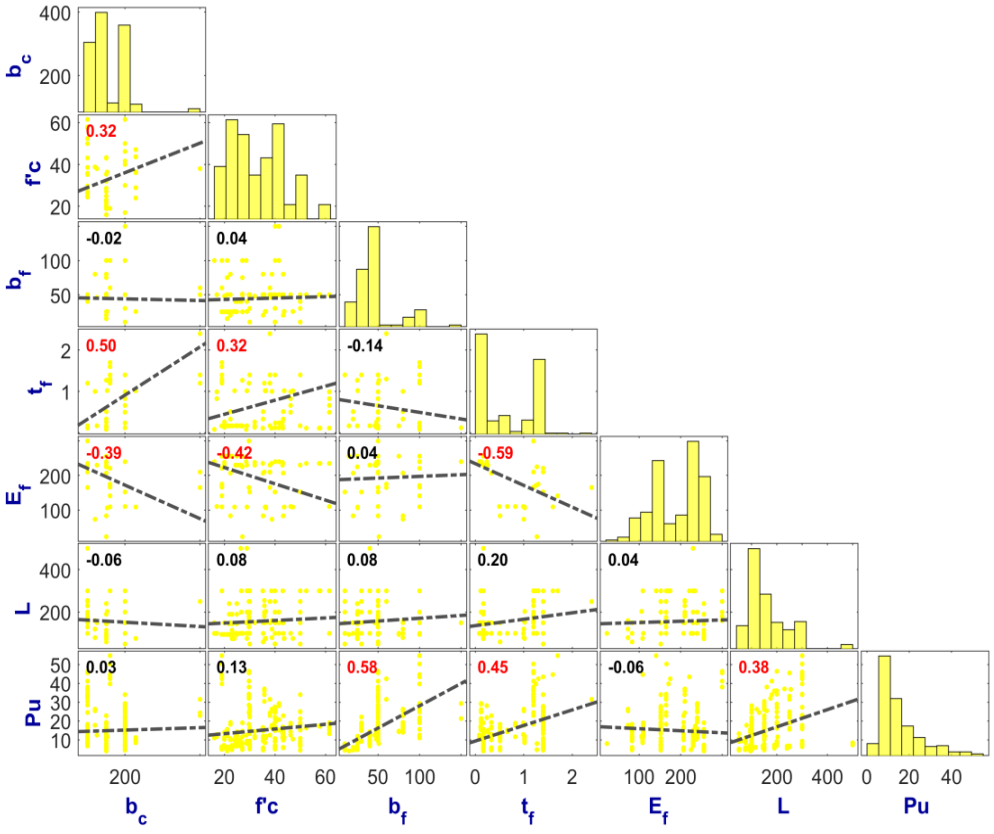

Fig. 3. Multi-correlation graph of input and output variables used in this study

4. Results and Discussion

4.1. Prediction capability

The ANFIS model and the ANFIS-PSO model are suggested in this work to forecast FRP-to-concrete bond strength. The process of building models depends on the selection of hyperparameters to obtain reliable and highly accurate outputs. Besides, the accuracy of ANFIS, or any machine learning algorithm, is highly dependent on the selection process of samples in the training dataset. In this step, the training dataset is divided into ten parts and subjected to a cross-validation process. With 10 simulations combined with trial and error, the final parameters selected for the ANFIS model and the PSO optimization algorithm are shown in Table 2.

Table 2. ANFIS and PSO parameters used in this study

	Values and Description
ANFIS parameters	
Input numbers	6
Output number	1
Type of membership function	Gaussian
Parameters per membership function	2
Membership function per input	8
Nonlinear parameter numbers	96
Linear parameter number	56
Total parameters	152
PSO parameters	
Swarm size	30
Maximum number of iterations	1000
Inertia weight	0.4
Personal learning coefficient	1
Global learning coefficient	2
Maximum velocity	5
Minimum velocity	-5

The average performance of the chosen models on the training and testing datasets is computed and reported in Fig 4. It is found that the ANFIS-PSO hybrid machine learning model exhibits better predictive performance than the ANFIS model. This is reflected in the higher R-value of the ANFIS-PSO model and lower RMSE and MAE values compared to the ANFIS model, for both training and testing datasets. Specifically, with the training dataset, the RMSE value fluctuates in the range of [2.15; 4.6] for the ANFIS-PSO model and [3.85; 4.85] for the ANFIS model. The MAE values corresponding to the ANFIS-PSO and ANFIS models vary in the ranges of [1.5; 3.55] and [2.75; 3.6], respectively. The values of R vary in the range of [0.885; 0.976] and [0.87; 0.926] for ANFIS-PSO and ANFIS models, respectively. With the testing dataset, the RMSE, MAE and R values corresponding to the ANFIS-PSO model range from [3.15; 5.45], [1.98; 3.4] and [0.865; 0.953], while with the ANFIS model, these values are in the range [4.1; 6.05], [3.2; 4.9] and [0.825; 0.89], respectively. The collected findings demonstrate that the two suggested models effectively predict the bond strength of FRP panels in concrete. Additionally, the results of 10-fold cross-validation demonstrate that the two models were constructed with a high degree of accuracy and dependability.

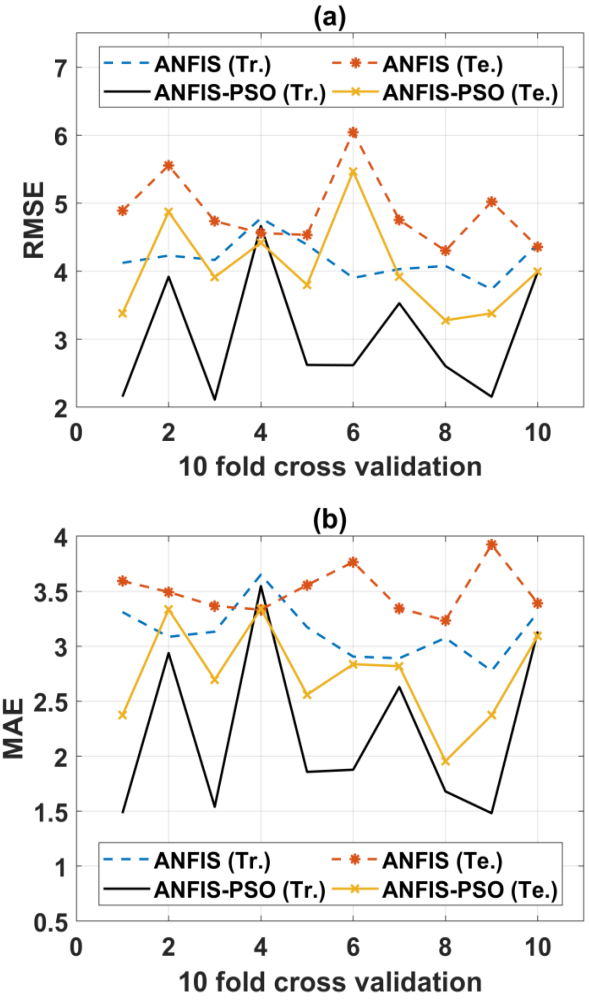

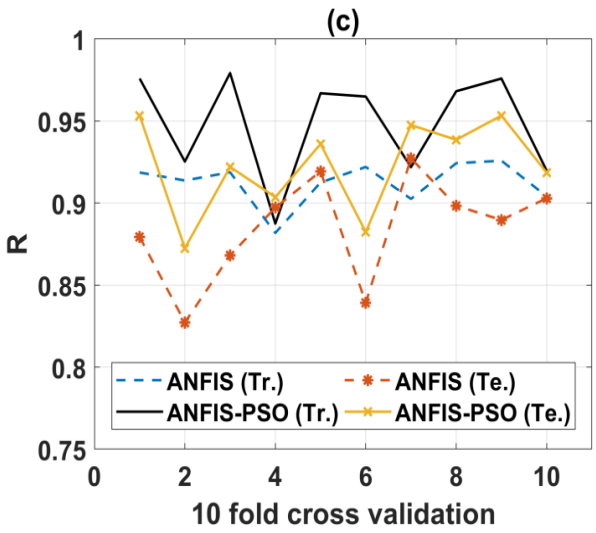

Fig. 4. Predictive performance results of ANFIS and ANFIS-PSO models correspond to 10 fold cross-validation based on the following criteria: (a) RMSE, (b) MAE, and (c) R

4.2. Typical prediction results

This section presents typical prediction results of ANFIS-PSO and ANFIS models, which are extracted from the models that have been built, validated, and verified in the previous section. Fig 5 illustrates the actual and anticipated bond strengths of FRP slabs in concrete when employing the ANFIS-PSO and ANFIS models, where solid lines indicate the experimental values and red and black dashed lines, respectively, reflect the expected values. As can be shown, the target values for 169 samples in the training dataset are very near to the observed values (Fig 5a). The remaining samples (73 experimental outcomes) in the testing dataset are likewise predicted with minimal errors (Fig 5b).

The regression graphs for the training and testing datasets, predicted by ANFIS-PSO and ANFIS are shown in Fig 6. It is shown that they are two perfect machine learning models to predict the bond strength of FRP-to-concrete with high accuracy. Specifically, the ANFIS-PSO model achieves R = 0.976, RMSE = 2,155, and MAE = 1.482 for the training dataset, and R = 0.953, RMSE = 3.381, and MAE = 2,373 for the test dataset. In addition, the ANFIS model achieves R = 0.926, RMSE = 3,734, and MAE = 10.91 for the training dataset, and R = 0.89, RMSE = 5.021, and MAE = 3.923 for the testing dataset. The results show that the ANFIS-PSO exhibits higher R values, lower MAE and RMSE values compared with ANFIS, which clearly shows the superior predictive performance of ANFIS-PSO model. Both presented models, however, are strong predictive models and perform well in general when estimating the bond strength of FRP to concrete.

Finally, in order to be more specific, Fig 7 shows the simulation error distribution of the ANFIS (Fig 7a) and ANFIS-PSO models (Fig 7b) through the training and testing datasets. As can be observed, both models' errors are highly clustered around the 0 kN location, which corresponds to the training and testing data sets. Only a few data with errors outside the range ± 10 kN are observed. The findings demonstrate that the proposed ANFIS and ANFIS-PSO models accurately predict the bond strength of FRP-to-concrete.

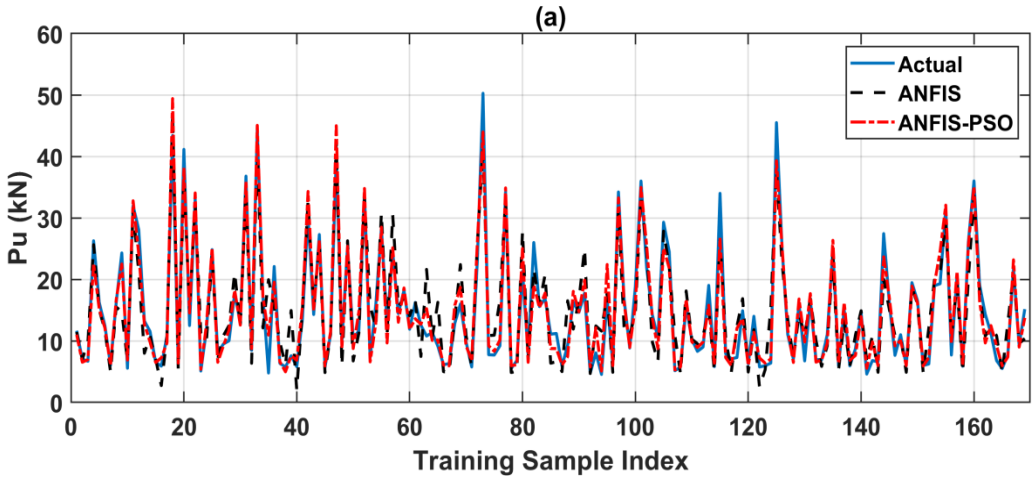

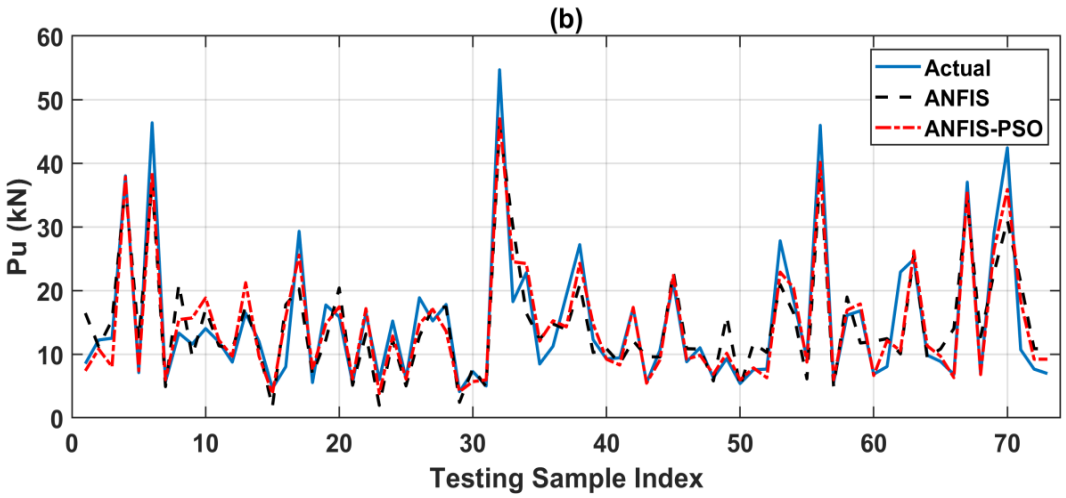

Fig. 5. Comparison of the performance of ANFIS and ANFIS-PSO with the actual values of Pu in function of (a) training dataset, (b) testing dataset

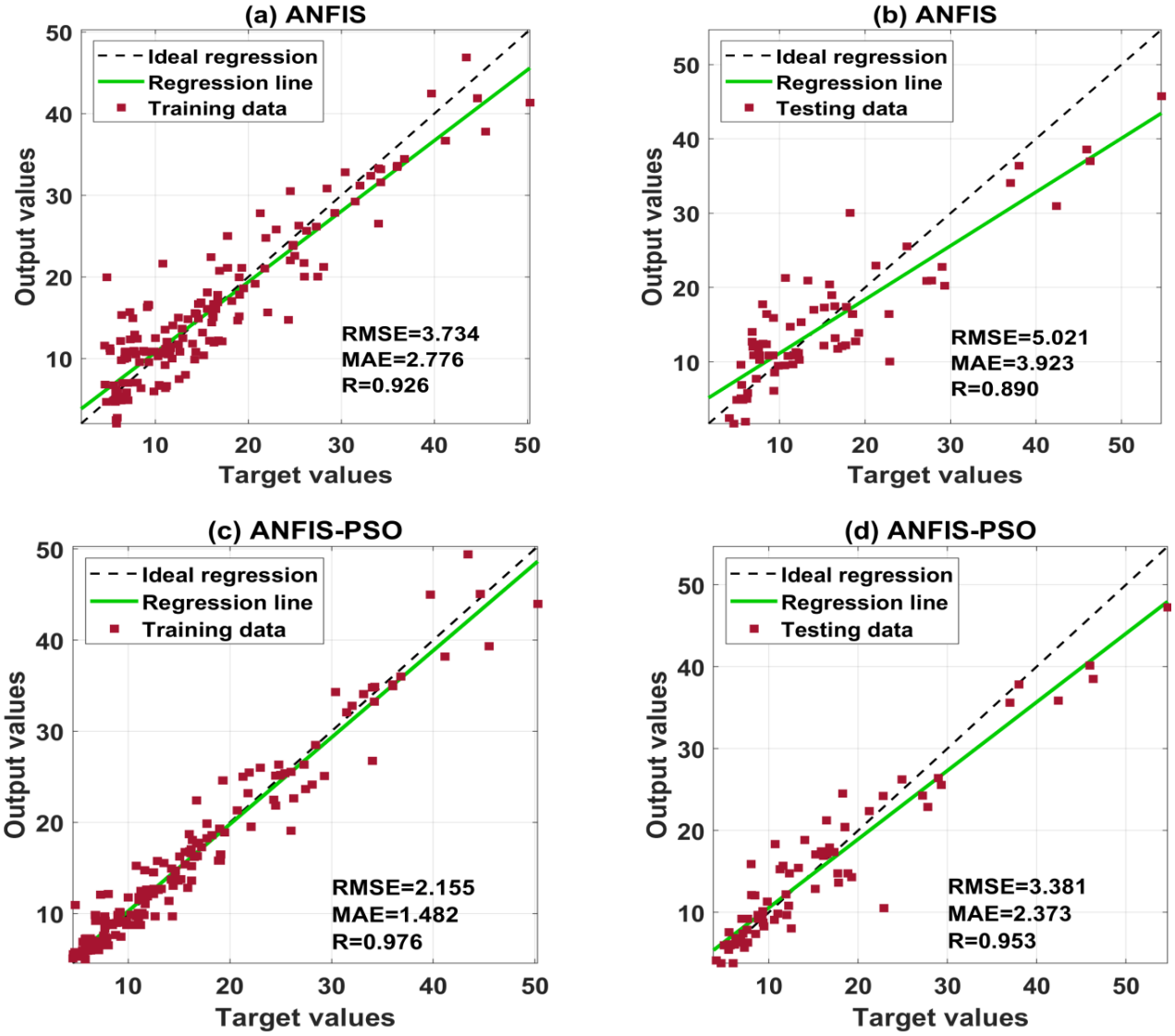

Fig. 6. Regression graphs showing the correlation between the target and output values for (a) ANFIS training dataset, (b) ANFIS testing dataset, (c) ANFIS-PSO training dataset, and (d) ANFIS-PSO testing dataset

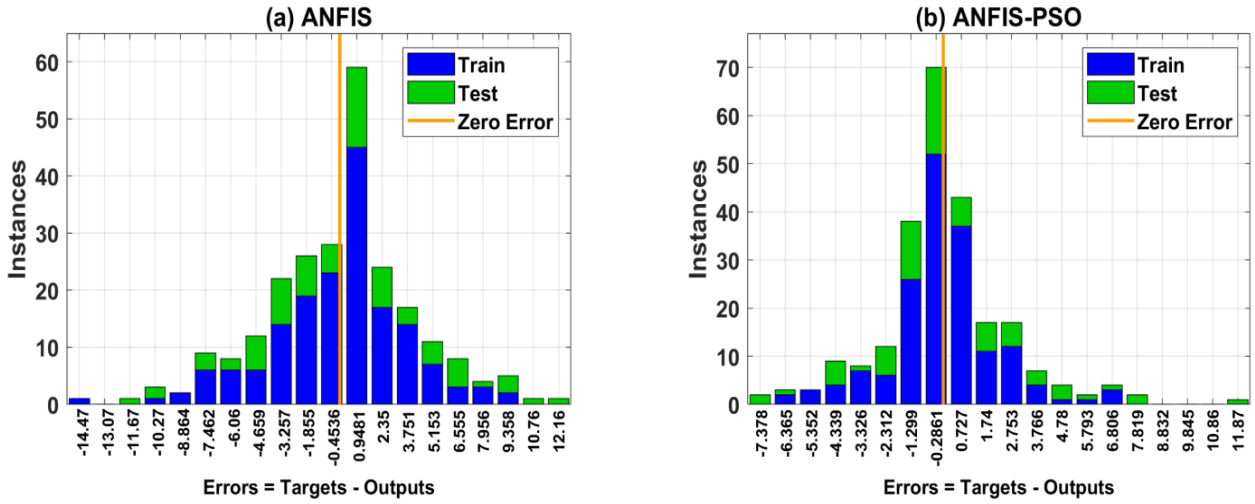

Fig. 7. Error distribution results of two models for training and testing dataset (a) ANFIS model

5. Conclusion

In this work, an Adaptive Neuro-Based Fuzzy Inference System (ANFIS) and a Particle Swarm Optimization (PSO) method are utilized to forecast the bond strength between the concrete surface and FRP sheets without using direct pull out stress. The ANFIS and ANFIS-PSO models are built utilizing a dataset of 242 test specimens obtained from different sources. Six input parameters are used to create the model: beam width, concrete compressive strength, FRP thickness, FRP modulus of elasticity, FRP length, and FRP width. Common statistical measures such as R, RMSE, and MAE are used to evaluate the performance of ANFIS and ANFIS-PSO models. This model predicts the bond strength with good dependability (R = 0.953, RMSE = 3.381, and MAE = 2.373 for the ANFIS-PSO model, R = 0.89, RMSE = 5.021, and MAE = 3.923 for the ANFIS model). The findings of this study would enable engineers to easily forecast the bond strength of FRP to concrete, which is beneficial throughout the calculation and design stages.

References

[1] R.H. Haddad, A.A. Al Dalou. (2018). Experimental study on bond behavior between corrosion-cracked reinforced concrete and CFRP sheets. *Journal of Adhesion Science and Technology*, 32(6), 590-608.

[2] J.G. Teng, J.F. Chen, S.T. Smith, L. Lam. (2003). Behaviour and strength of FRP-strengthened RC structures: a state-of-the-art review. *Proceedings of the Institution of Civil Engineers – Structures and Buildings*, 156(1), 51-62.

[3] C.E. Bakis, L.C. Bank, Vl. Brown, E. Cosenza, J.F. Davalos, J.J. Lesko, A. Machida, S.H. Rizkalla, T.C. Triantafillou. (2002). Fiber-reinforced polymer composites for construction—State-of-the-art review. *Journal of Composites for Construction*, 6(2), 73-87.

[4] S.M. Hamze-Ziabari, A. Yasavoli. (2017). Predicting Bond Strength between FRP Plates and Concrete Substrate: Applications of GMDH and MNLR Approaches. *Journal of Advanced Concrete Technology*, 15, 644-661.

[5] Z.S. Wu, H. Yoshizawa. (1999). Analytical/experimental study on composite behavior in strengthening structures with bonded carbon fiber sheets. Journal of Reinforced Plastics and Composites, 18(12), 1131-1155.

[6] J. Yao, J.G. Teng, J.F. Chen. (2005). Experimental study on FRP-to-concrete bonded joints. *Composites Part B: Engineering*, 36(2), 99-113.

[7] M.J. Chajes, W.W. Finch, T.A. Thomson. (1996). Bond and force transfer of composite-material plates bonded to concrete. *Structural Journal*, 93(2), 209-217.

[8] S.K. Sharma, M.S.M. Ali, D. Goldar, P.K. Sikdar.

(2006). Plate–concrete interfacial bond strength of FRP and metallic plated concrete specimens. *Composites Part B: Engineering*, 37(1), 54-63.

[9] M. Malena, G. de Felice. (2014). Debonding of composites on a curved masonry substrate: Experimental results and analytical formulation. *Composite Structures*, 112, 194-206.

[10] X.Z. Lu, L.P. Ye, J.G. Teng, J.J. Jiang. (2005). Meso-scale finite element model for FRP sheets/plates bonded to concrete. *Engineering Structures*, 27(4), 564-575.

[11] P. Carrara, D. Ferretti. (2013). A finite-difference model with mixed interface laws for shear tests of FRP plates bonded to concrete. *Composites Part B: Engineering*, 54, 329-342.

[12] J. Dai, T. Ueda, Y. Sato. (2005). Development of the nonlinear bond stress–slip model of fiber reinforced plastics sheet–concrete interfaces with a simple method. *Journal of Composites for Construction*, 9(1), 52-62.

[13] J. Dai, T. Ueda, Y. Sato. (2006). Unified analytical approaches for determining shear bond characteristics of FRP-concrete interfaces through pullout tests. *Journal of Advanced Concrete Technology*, 4(1), 133-145.

[14] J.F. Chen, J.G. Teng. (2001). Anchorage strength models for FRP and steel plates bonded to concrete. *Journal of Structural Engineering*, 127(7), 784-791.

[15] B.B. Adhikary, H. Mutsuyoshi. (2001). Study on the bond between concrete and externally bonded CFRP sheet. FRPRCS-5 Fibre-Reinf. Plast. Reinf. Concr. Struct. Vol. 1 Proc. Fifth Int. Conf. Fibre-Reinf. Plast. Reinf. Concr. Struct. Camb. UK 16–18, Thomas Telford Publishing, pp 371-378.

[16] U.S. Camli, B. Binici. (2007). Strength of carbon fiber reinforced polymers bonded to concrete and masonry. *Construction and Building Materials*, 21(7), 1431-1446.

[17] T. D'Antino, C. Pellegrino. (2014). Bond between FRP composites and concrete: Assessment of design procedures and analytical models. *Composites Part B: Engineering*, 60, 440-456.

[18] H.M. Diab, O.A. Farghal. (2014). Bond strength and effective bond length of FRP sheets/plates bonded to concrete considering the type of adhesive layer. *Composites Part B: Engineering*, 58, 618-624.

[19] S. Ueno, H. Toutanji, R. Vuddandam. (2015). Introduction of a stress state criterion to predict bond strength between FRP and concrete substrate. *Journal of Composites for Construction*, 19(1) 04014024.

[20] H.-B. Ly, T.-T. Le, H.-L.T. Vu, V.Q. Tran, L.M. Le, B.T. Pham. (2020). Computational Hybrid Machine Learning Based Prediction of Shear Capacity for Steel Fiber Reinforced Concrete Beams. *Sustainability*, 12(7), 2709.

[21] H.-B. Ly, B.T. Pham, L.M. Le, T.-T. Le, V.M. Le, P.G. Asteris. (2021). Estimation of axial load-carrying capacity of concrete-filled steel tubes using surrogate models. *Neural Computing and Applications*, 33(8), 3437-3458.

[22] H.-B. Ly, T.-A. Nguyen, V.Q. Tran. (2021). Development of deep neural network model to predict the compressive strength of rubber concrete. *Construction and Building Materials*, 301, 124081.

[23] H.-B. Ly, M.H. Nguyen, B.T. Pham. (2021). Metaheuristic optimization of Levenberg–Marquardt-based artificial neural network using particle swarm optimization for prediction of foamed concrete compressive strength. *Neural Computing and Applications*, 33, 17331-17351.

[24] T.-A. Nguyen, H.-B. Ly, B.T. Pham. (2020). Backpropagation Neural Network-Based Machine Learning Model for Prediction of Soil Friction Angle. *Mathematical Problems in Engineering*, 2020, 8845768, 1-11.

[25] B.T. Pham, M.D. Nguyen, H.-B. Ly, T.A. Pham, V. Hoang, H.V. Le, T.-T. Le, H.Q. Nguyen, G.L. Bui. (2020). Development of Artificial Neural Networks for Prediction of Compression Coefficient of Soft Soil. C. Ha-Minh, D.V. Dao, F. Benboudjema, S. Derrible, D.V.K. Huynh, A.M. Tang (Eds.), CIGOS 2019

Innov. Sustain. Infrastruct., Springer Singapore, pp 1167-1172.

[26] J.-S.R. Jang. (1993). ANFIS: adaptive-network-based fuzzy inference system. *IEEE Transactions on Systems, Man, and Cybernetics*, 23(3), 665-685.

[27] M.A. Boyacioglu, D. Avci. (2010). An adaptive network-based fuzzy inference system (ANFIS) for the prediction of stock market return: the case of the Istanbul stock exchange. *Expert Systém with Applications*, 37(12), 7908-7912.

[28] J. Kennedy, R. Eberhart. (1995). Particle swarm optimization. Proc. ICNN95-Int. Conf. Neural Netw., IEEE, pp 1942-1948.

[29] Y. Jung, J. Hu. (2015). A K-fold averaging cross-validation procedure. *Journal of Nonparametric Statistics*, 27(2), 167-179.

[30] B.G. Marcot, A.M. Hanea. (2020). What is an optimal value of k in k-fold cross-validation in discrete Bayesian network analysis?, *Computational Statistics*, 52(5), 667-692.

[31] B.T. Pham, T.V. Phong, H.D. Nguyen, C. Qi, N. Al-Ansari, A. Amini, L.S. Ho, T.T. Tuyen, H.P.H. Yen, H.-B. Ly. (2020). A comparative study of kernel logistic regression, radial basis function classifier, multinomial naïve bayes, and logistic model tree for flash flood susceptibility mapping. *Water*, 12(1), 239.

[32] H.-B. Ly, P.G. Asteris, T.B. Pham. (2020). Accuracy assessment of extreme learning machine in predicting soil compression coefficient. *Vietnam Journal of Earth Sciences*, 42(3) 228-336.

[33] C. Qi, H.-B. Ly, L.M. Le, X. Yang, L. Guo, B.T. Pham. (2021). Improved strength prediction of cemented paste backfill using a novel model based on adaptive neuro fuzzy inference system and artificial bee colony. *Construction and Building Materials*, 284, 122857.

[34] K. Takeo, H. Matsushita, T. Makizumi, G. Nagashima. (1997). Bond characteristics of CFRP sheets in the CFRP bonding technique. *Proceedings of the Japan Concrete Institute*, 19, 1599-1604.

[35] S.-K. Woo, Y. Lee. (2010). Experimental study on interfacial behavior of CFRP-bonded concrete. *KSCE Journal of Civil Engineering*, 14, 385-393.

[36] M. Zhao, F. Ansari. (2004). Bond properties of FRP fabrics and concrete joints. 13th World Conference on Earthquake Engineering Vancouver, B.C., Canada, 35.

[37] D. Mostofinejad, M.H. Mofrad, A. Hosseini, H.H. Mofrad. (2018). Investigating the effects of concrete compressive strength, CFRP thickness and groove depth on CFRP-concrete bond strength of EBROG joints. *Construction and Building Materials*, 189, 323-337.

[38] M. Ali-Ahmad, K. Subramaniam, M. Ghosn. (2006). Experimental investigation and fracture analysis of debonding between concrete and FRP sheets. *Journal of Engineering Mechanics*, 132(9), 914-923.

[39] M.H. Al-Allaf, L. Weekes, L. Augusthus-Nelson, P. Leach. (2016). An experimental investigation into the bond-slip behaviour between CFRP composite and lightweight concrete. *Construction and Building Materials*, 113, 15-27.

[40] J. Pan, C.K. Leung. (2007). Effect of concrete composition on FRP/concrete bond capacity. *Journal of Composites for Construction*, 11(6), 611-618.

[41] C. Czaderski, K. Soudki, M. Motavalli. (2010). Front and side view image correlation measurements on FRP to concrete pull-off bond tests. *Journal of Composites for Construction*, 14(4), 451-463.

[42] C. Mazzotti, B. Ferracuti, A. Bilotta, F. Ceroni, E. Nigro, M. Pecce. (2012). Sensitivity of FRP-concrete bond behavior to modification of the experimental set-up. *VI International Conference on FRP Composites in Civil Engineering*.